

## CHAPTER III

### RESULTS AND DISCUSSION

#### 3.1 Characterization

##### 3.1.1 FTIR Spectrophotometry

The FTIR spectrum of the synthesized DBSA-doped polypyrrole is compared with spectrum of neutral, undoped polypyrrole as reported by *Street et al. (1982)* shown in Figure 3.1. The spectrum of DBSA-doped polypyrrole shows a featureless decrease in absorption from 4000  $\text{cm}^{-1}$  to 1600  $\text{cm}^{-1}$ . The NH and CH bands, which should be observed at 3400  $\text{cm}^{-1}$  and  $\sim 3000$   $\text{cm}^{-1}$ , respectively, are not visible because they are masked by the tail of the  $\sim 1$  eV ( $\sim 8066$   $\text{cm}^{-1}$ ) peak representing the bipolaron absorption observed in the near-IR region. This characteristic is a well-known signature for the electrical conductivity of every conductive polymers. The  $\sim 1$  eV peak is absent in the neutral form of the polypyrrole (Figure 3.1a), so the NH and CH bands can be seen. The regions below 1600  $\text{cm}^{-1}$  are similar for both oxidized and neutral polymers because they contain the same pyrrole moiety. The bands at 1560  $\text{cm}^{-1}$  and 1531  $\text{cm}^{-1}$  identifying the asymmetrical and symmetrical double bond vibrations in pyrrole rings can be observed. The bands at 1150  $\text{cm}^{-1}$  and 620  $\text{cm}^{-1}$  represent the S=O and S-O stretching of the sulfate anions which compensated the positive charges in the polypyrrole chains.

To study the effect of the doping level of the conductive polymer on the electrical property and sensitivity to the certain gas, the DBSA-doped polypyrroles were synthesized by varying the DBSA concentrations that acted as the dopant from 1.5 - 4.0 M. Figure 3.2 shows the FTIR spectra with various

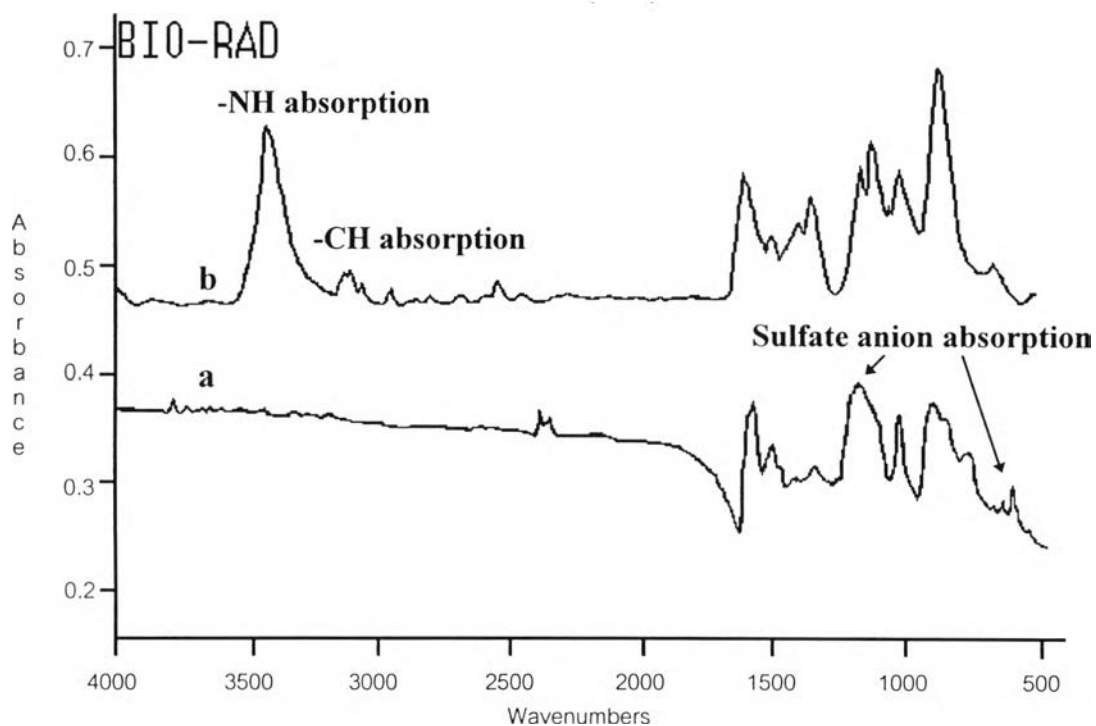


**Figure 3.1** The FTIR spectra of (a) the DBSA-doped polypyrrole and (b) neutral, undoped polypyrrole.

DBSA concentrations. We found that the absorption bands of sulfate anions, observed at  $1150 \text{ cm}^{-1}$  and  $620 \text{ cm}^{-1}$ , increase in their intensities with the increase in DBSA concentrations. This result implies that more DBSA molecules can interact with the polypyrrole chains when higher DBSA concentrations are used.

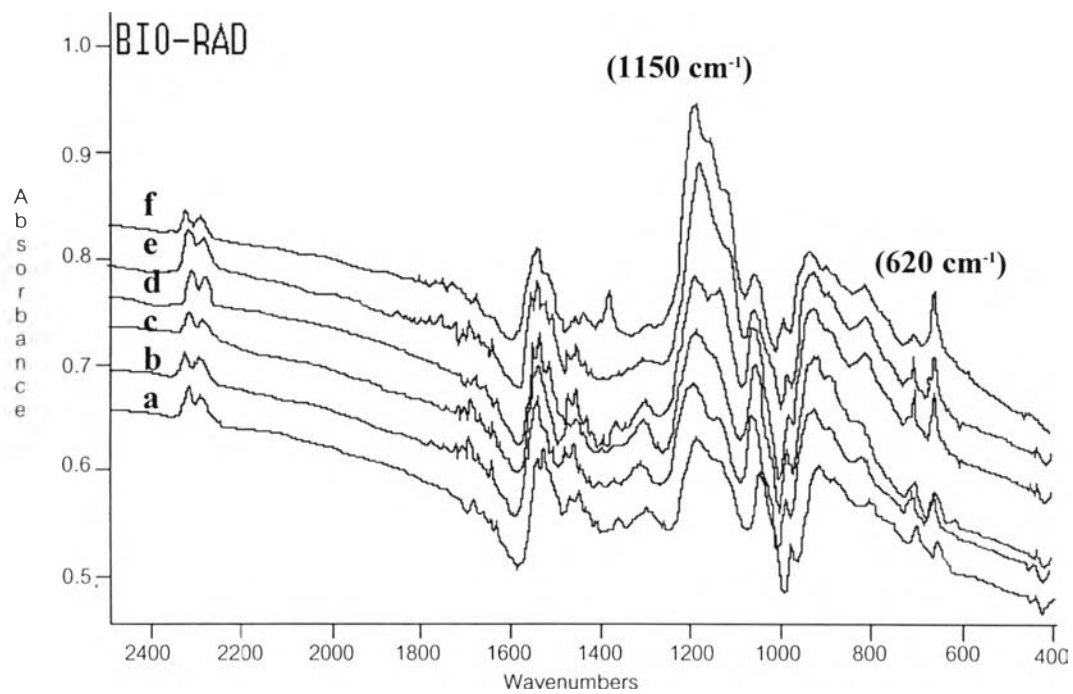


**Figure 3.2** The FTIR spectra of the DBSA-doped polypyrrole prepared by using DBSA concentrations of (a) 1.5 M , (b) 2.0 M , (c) 2.5 M , (d) 3.0 M , (e) 3.5 M and (f) 4.0 M.

### 3.1.2 Elemental Analysis

Figure 3.3 shows a plot of the doping level of DBSA-doped polypyrrole calculated from S/N weight ratio analyzed by elemental analyzer in CHNS mode using Equation 2.1 as a function of DBSA concentration. In this experiment, we varied the DBSA concentration from 0.12 M to 4.5 M. We found that the doping level increases with the DBSA concentration. The results agree with the FTIR spectra which show the increase in the magnitude of sulfate anion absorption and confirm that more DBSA molecules penetrate into the polypyrrole chains when higher DBSA concentration are used.

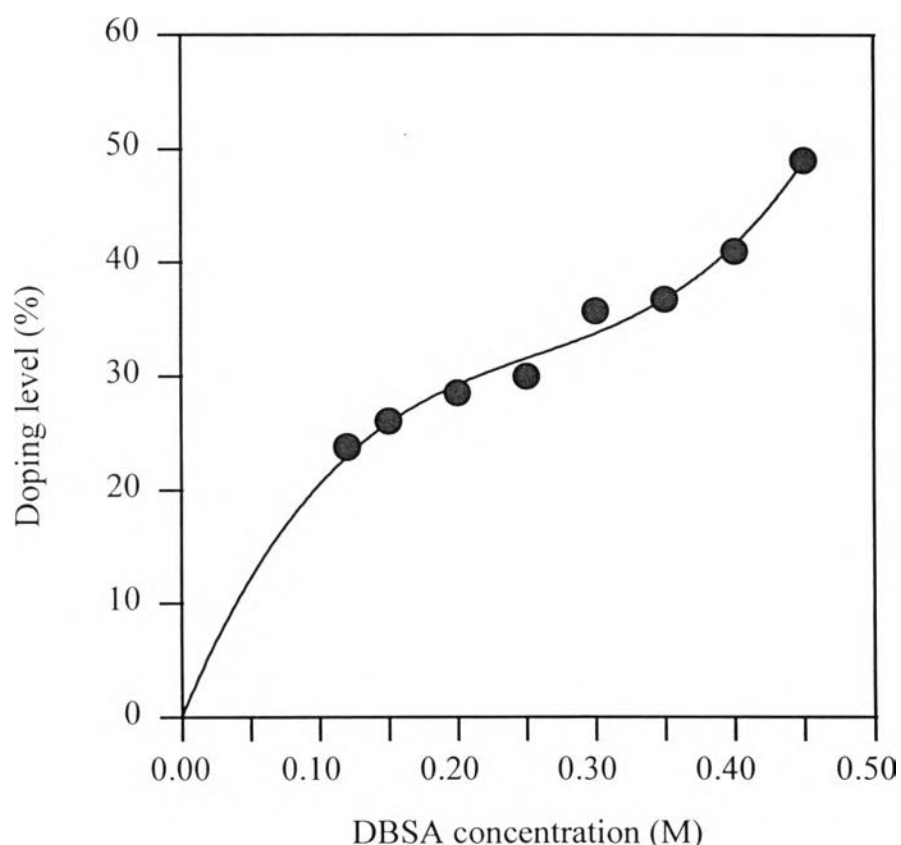


**Figure 3.3** Plot of the doping level as the function of DBSA concentration.

The results of elemental analysis of DBSA-doped polypyrrole not only give the effect of the doping level data but also roughly provide chemical structure information. The chemical structure is indicated by observing atom mole ratio of each element (C, H, N, S and O). The atom mole ratios of the elements were calculated by dividing the weight ratio by each molecular weight and then normalizing with one nitrogen atom. The oxygen contents were determined by difference with weight of C, H, N and S obtained from the elemental analysis. This calculation is shown in Appendix C and the atom mole ratios of DBSA-doped polypyrrole prepared by using various DBSA concentrations are shown in Table 3.1.

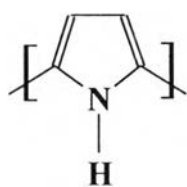
**Table 3.1 Atom mole ratios from elemental analyzer of DBSA-doped polypyrrole with various DBSA concentrations**

[DBSA] (M)	Pyrrole Ring <sup>a</sup>			Anion <sup>a</sup> (C <sub>18</sub> H <sub>29</sub> O <sub>3</sub> S)				Excess Oxygen <sup>b</sup>
	C	H	N	C	H	S	O	
0.12	4.00	5.233	1.00	4.307	6.900	0.238	0.714	0.997
0.15	4.00	5.278	1.00	4.662	7.539	0.260	0.780	0.754
0.20	4.00	5.490	1.00	5.134	8.266	0.285	0.855	0.461
0.25	4.00	5.399	1.00	5.399	8.687	0.300	0.899	0.020
0.30	4.00	5.612	1.00	6.431	10.352	0.357	1.071	0.613
0.35	4.00	5.589	1.00	6.623	10.667	0.368	1.103	0.722
0.40	4.00	5.708	1.00	7.390	11.883	0.410	1.229	0.906
0.45	4.00	5.803	1.00	8.824	14.207	0.490	1.470	0.403

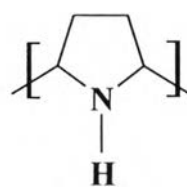
Note : a : They were normalized to N atom.

b : They were obtained by difference.

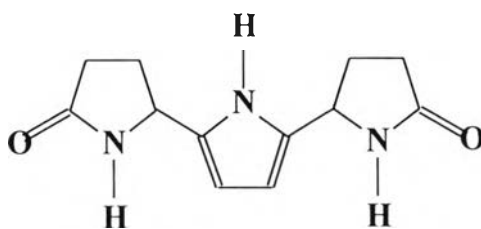
Table 3.1, shows that excess hydrogen and oxygen were contained in the samples. *Salmon et al. (1982)* reported that these excesses indicated that the polypyrrole was not simply a linear chain with pyrrole units but also contained some saturated pyrrolidine units and/or partially saturated units terminated with pyrrolidinone structures as shown in Figure 3.4.



Pyrrole unit



Pyrrolidine unit



Pyrrolidinone structures

**Figure 3.4** The proposed chemical structures of polypyrrole.

### 3.1.3 UV-VIS Spectrophotometry

UV-VIS spectra were studied because they show an optical property that is important for the conductive polymers. The optical property of the conductive polymer frequently considered is the absorption wavelength in electron volt units which can be converted to photon energy in electron volt units by using Einstein's equation as expressed in Equation 2.2. Figure 3.5 is the UV-VIS spectra of 1 g / 100 ml m-cresol solution of DBSA-doped polypyrrole at different doping levels : 0.15 M, 0.30 M and 0.40 M of DBSA, representing the low, medium and high doping levels of DBSA-doped polypyrroles, respectively. It can be seen that there appear two absorption

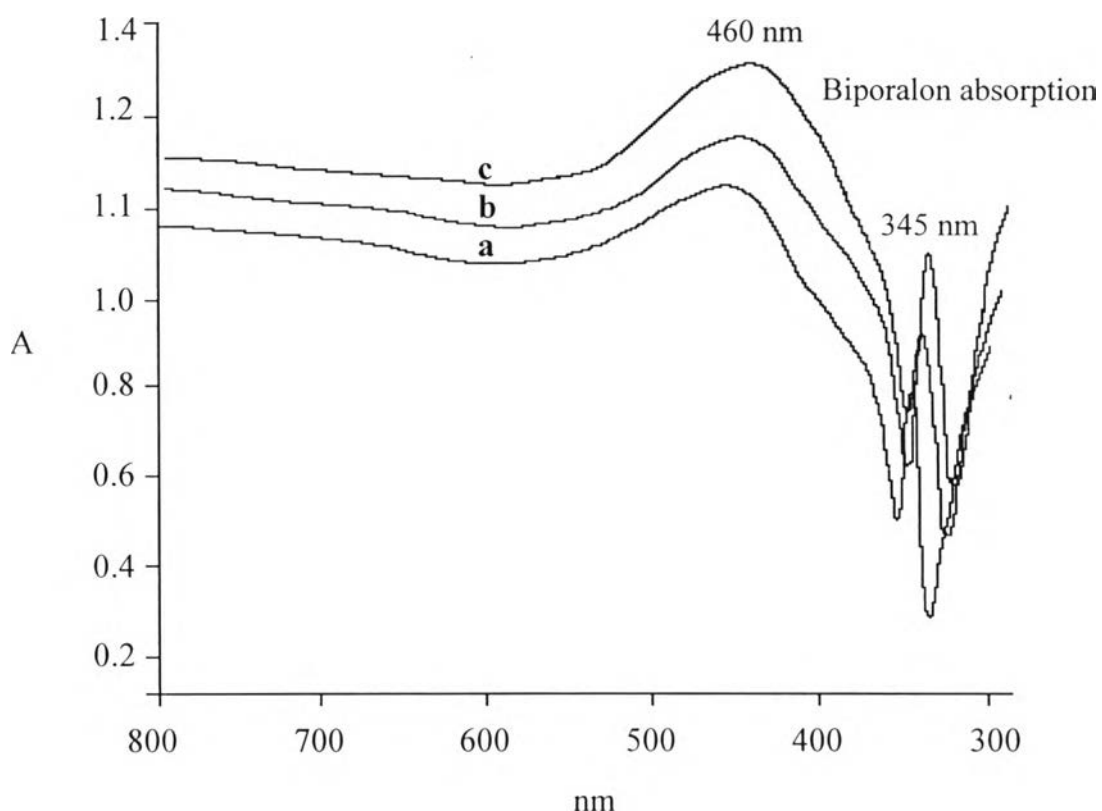


**Figure 3.5** UV-VIS spectra of m-cresol solution of polypyrrole doped by DBSA concentration (a) 0.15 M, (b) 0.20 M, (c) 0.40 M.

peaks at 345 nm and 460 nm, on energy levels of 3.6 eV and 2.7 eV, respectively. These two absorptions are interpreted as evidence for the presence of bipolaron states in polypyrrole chains that indicate the conducting behavior of the polymer.

*Yakushi et al. (1983)* showed the absorption spectra of polypyrrole perchlorate films together with the spectra of a series of such films subjected to various doping levels. They reported a Blue shift from 2.1 eV and 3.2 eV peaks to 2.7 eV and 3.6 eV peaks, respectively, upon increasing the doping level, but we cannot find this event in our result. The reason might be the narrow variation of doping level used in our work. In the synthesis of soluble polypyrrole by using Lee's method, the possible range of DBSA concentration that we were able to use was only from 0.15 to 0.45 M because of the solubility fixes the lower limit and processibility sets the upper limit.



### 3.1.4 SEM

In our present investigation, SEM was used to measure the film thickness and to study the morphology of the synthesized DBSA-doped polypyrroles. The results were divided into two parts :

*3.1.4.1 Film Thickness Determination.* SEM was needed to observe the thickness of film because the prepared polypyrrole film was thin and rather brittle and they could not be separated from the substrate. DBSA-doped polypyrrole films used in the conductivity study were prepared as mentioned in the section 2.2.2. Figure 3.6 shows an example of SEM image in the edge view of the 0.30 M DBSA-doped polypyrrole film. The film thickness was measured by observing an edge view of the sample by using the standard scale setting in the SEM program. The obtained film thickness is an important parameter to calculate the specific conductivity as expressed in Equation 2.5.

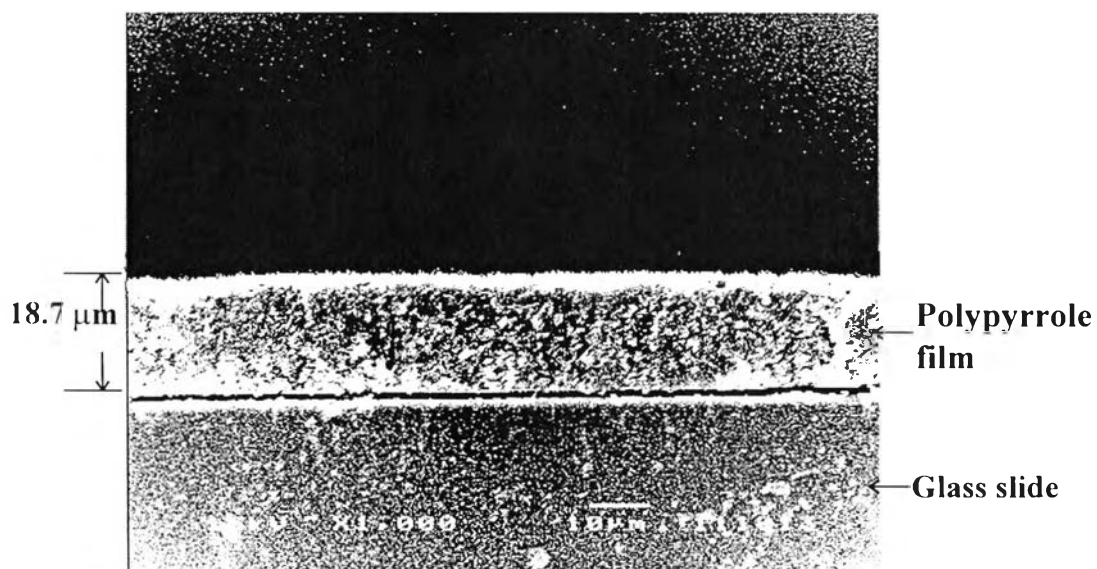
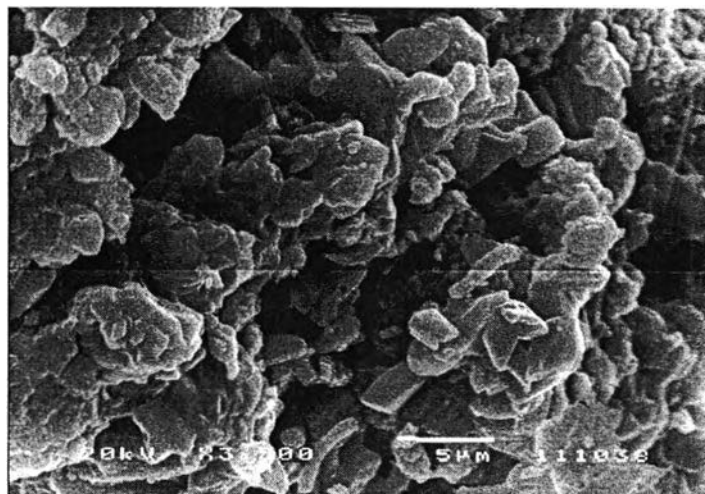


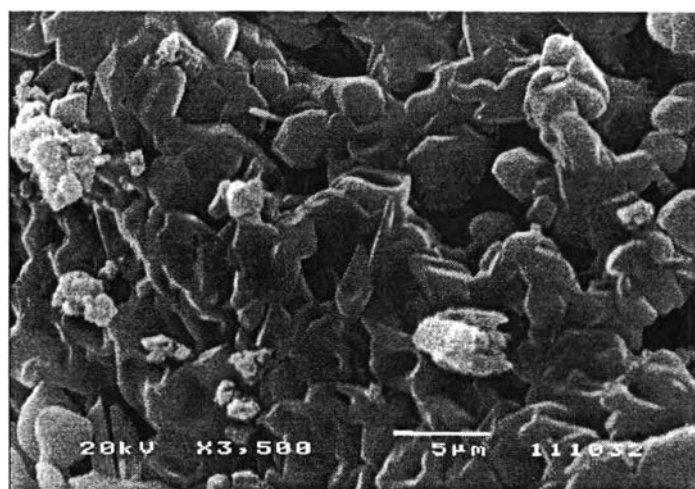
**Figure 3.6** SEM image in the edge view of the 0.30 M DBSA-doped polypyrrole film.

*3.1.4.2 Morphology.* The morphology of the polypyrrole can be easily influenced by the doping level. Shown in Figure 3.7 are the SEM micrographs (magnification 3,500 times) of the synthesized DBSA-doped polypyrrole with various DBSA concentrations. It is interesting to find that the morphology of DBSA-doped polypyrrole synthesized by the current method exhibits the change from the typical 3-D random coils, granular morphology, to the rigid rod-like, fibrillar morphology, upon the increase in DBSA concentration. Moreover, the amount and diameter of fibrils were seen to increase with DBSA concentration. More positive charges along the polypyrrole chains at the higher DBSA concentrations induce higher doping levels. The repulsing effect of the positive charges in the polymer chains causes the polymer chains to expand toward fibrillar forms.

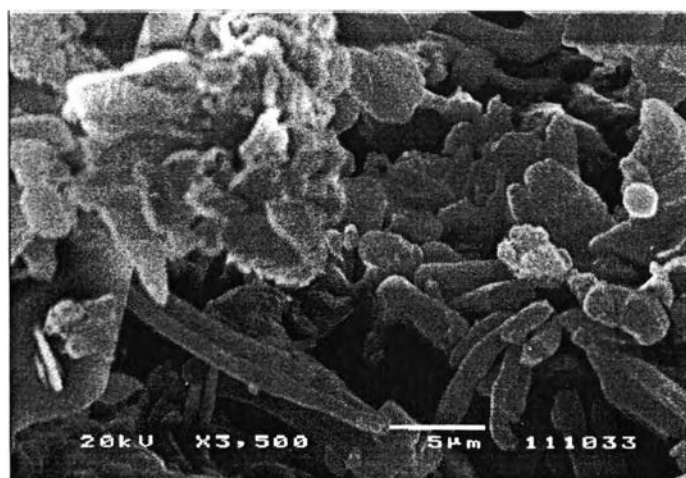
*Meixiang et al (1997)* showed that the polypyrrole prepared by chemical polymerization of pyrrole monomer in the presence of  $\beta$ -naphthalene sulfonic acid (NSA), as the dopant, exhibits the fibrillar morphology with a diameter of about 0.5  $\mu\text{m}$  whereas the synthesized DBSA-doped polypyrroles gave diameter of about 2.5 - 7.5  $\mu\text{m}$ . In addition, the polymerization conditions can significantly influence the morphology of the obtained polypyrroles.



a) 0.15 M DBSA

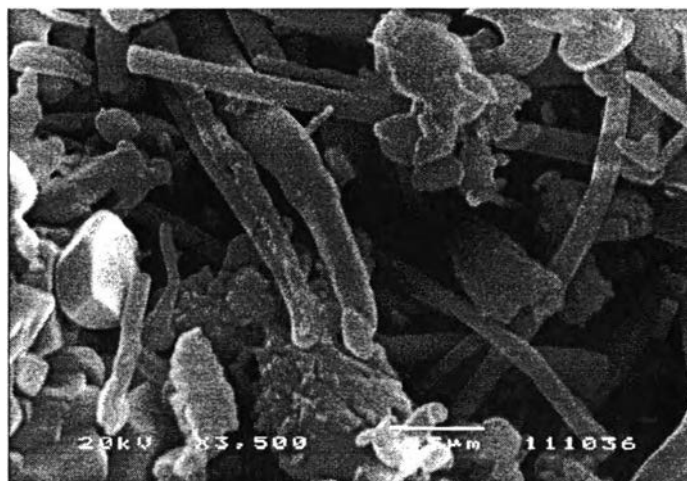


b) 0.20 M DBSA

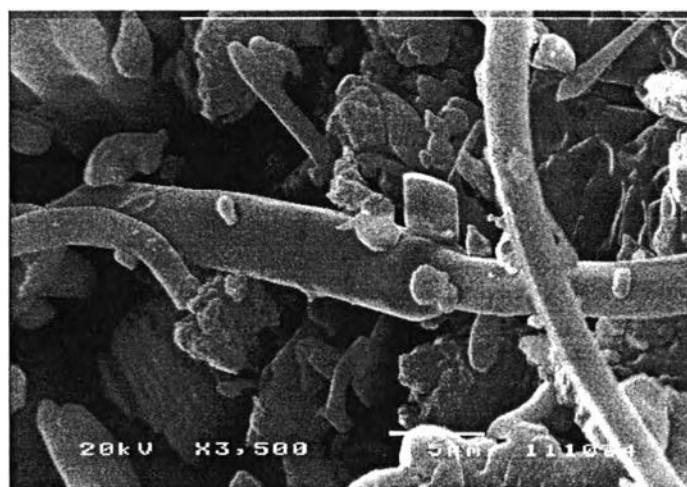


c) 0.25 M DBSA

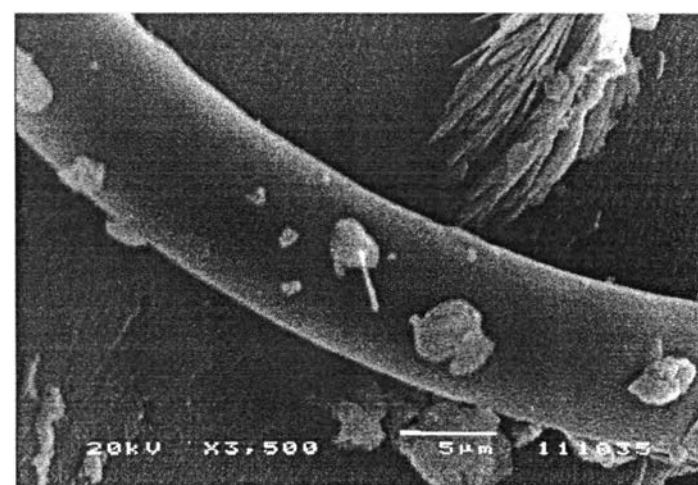
( continue )



d) 0.30 M DBSA



e) 0.35 M DBSA



f) 0.40 M DBSA

**Figure 3.7** SEM micrographs of the synthesized DBSA-doped polypyrrole with various DBSA concentrations. Magnification was 3,500 times

## 3.2 Preliminary Test

### 3.2.1 Effect of Aging Time on The Conductivity Response

To study the conductivity response of the synthesized DBSA-doped polypyrrole films in the equilibrium state, the effect of aging time was studied. The DBSA-doped polypyrrole films were stored in the dessicator before the detections of the specific conductivity by the four-point probe detector with an applied current of 2.7  $\mu\text{A}$  in 1 atm of  $\text{N}_2$  atmosphere at 18  $^\circ\text{C}$ . As shown in Figure 3.8, differently doped polypyrrole films show saturation states of the specific conductivity after 40 days, as a result of reactions with the oxygen in the environment and some humidity during storage.

The specific conductivity change ( $\Delta\sigma_{\text{dc}}$ ) was calculated by Equation 3.1 and recorded in Table 3.2.

$$\Delta\sigma_{\text{dc}} = \frac{\sigma_t - \sigma_o}{\sigma_o} \times 100 \quad (3.1)$$

where  $\sigma_o$  is the initial specific conductivity detected and  $\sigma_t$  is the specific conductivity detected after aging. We see that the conductivity change is a function of doping level; with a higher stability exhibited by polypyrrole having a higher doping level. From this test we decided to detect the conductivity after 40 days or in the equilibrium state of the conductivity response.

**Table 3.2** The conductivity change of the DBSA-doped polypyrrole films as a function of DBSA concentration

<b>DBSA concentration (M)</b>	<b><math>\Delta\sigma_{dc}</math> (%)</b>
0.15	164.92
0.20	215.70
0.25	156.53
0.30	96.89
0.35	37.56
0.40	35.63

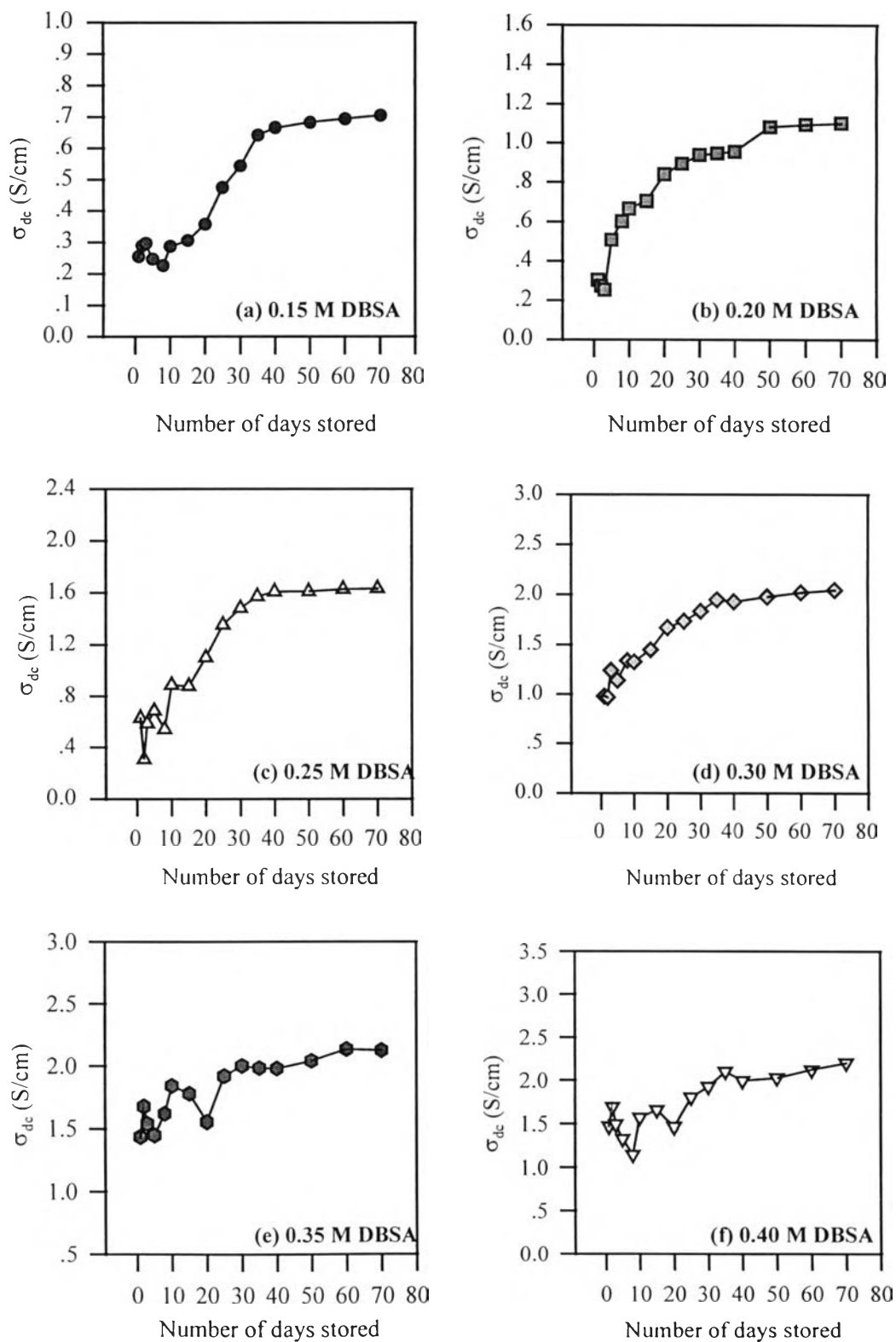


**Figure 3.8** Effect of aging time on the specific conductivity ( $\sigma_{dc}$ ) for the DBSA-doped polypyrroles of various DBSA concentrations.

### 3.2.2 Statistical Test

The statistical test was used to determine the reproducibility of the conductivity response of the DBSA-doped polypyrrole films detected by the four-point probe detector. In this test, two batches of polypyrrole were synthesized by using the same conditions (DBSA concentration = 0.30 M and APS = 0.06 mol). Then 10 polypyrrole films of each batch were prepared as described in the section 2.2.2 and the conductivity of those films were measured by four-point probe detector with an applied current of 2.7  $\mu\text{A}$  in 1 atm of  $\text{N}_2$  atmosphere at 18  $^\circ\text{C}$ . Average specific conductivity, standard deviation, control limit (mean  $\pm$  std.dev.), specification (mean  $\pm$  3 std.dev.), and the coefficients of variation were calculated and shown in Table 3.3. Figure 3.9 presents the X-bar charts of the specific conductivity for 0.3 M DBSA-doped polypyrrole films.

**Table 3.3 The statistical data of 0.30 M DBSA-doped polypyrrole films**

<b>Statistic Data</b>	<b>Batch 1 (S/cm)</b>	<b>Batch 2 (S/cm)</b>
Mean	2.0479	1.9949
Standard deviation	0.0518	0.0502
Control limit	1.9961-2.0997	1.9447-2.0451
Specification	1.8925-2.2033	1.8443-2.1455
% coefficient of variation	2.53	2.52

We can see that all data of both batches are within the specification limit and % coefficients of variation are acceptable to conclude that the conductivity responses detected from the four-point probe detector have an overall good reproducibility.



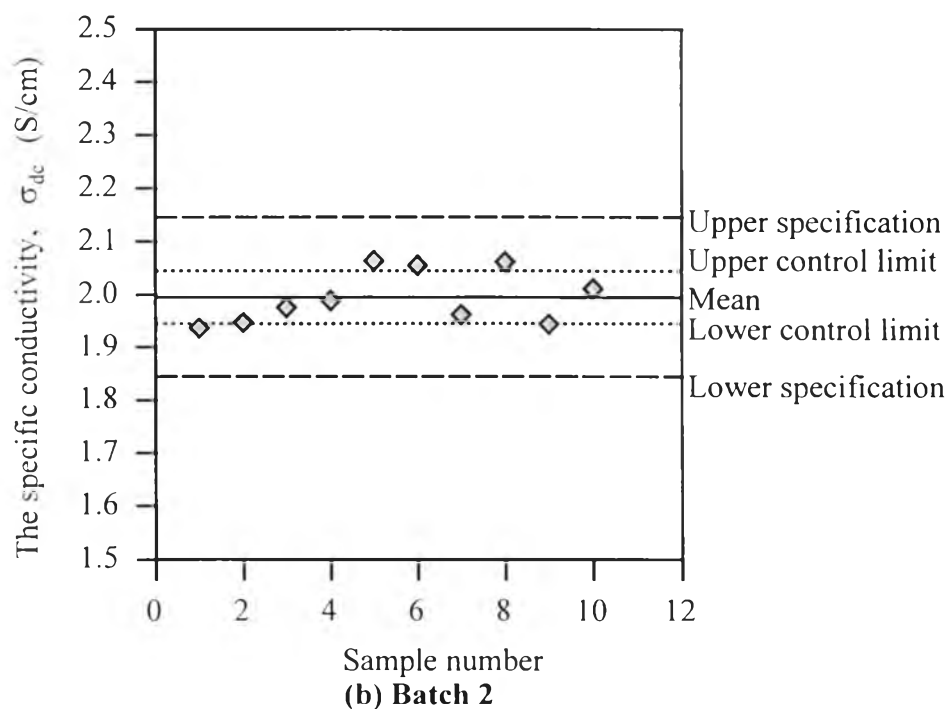
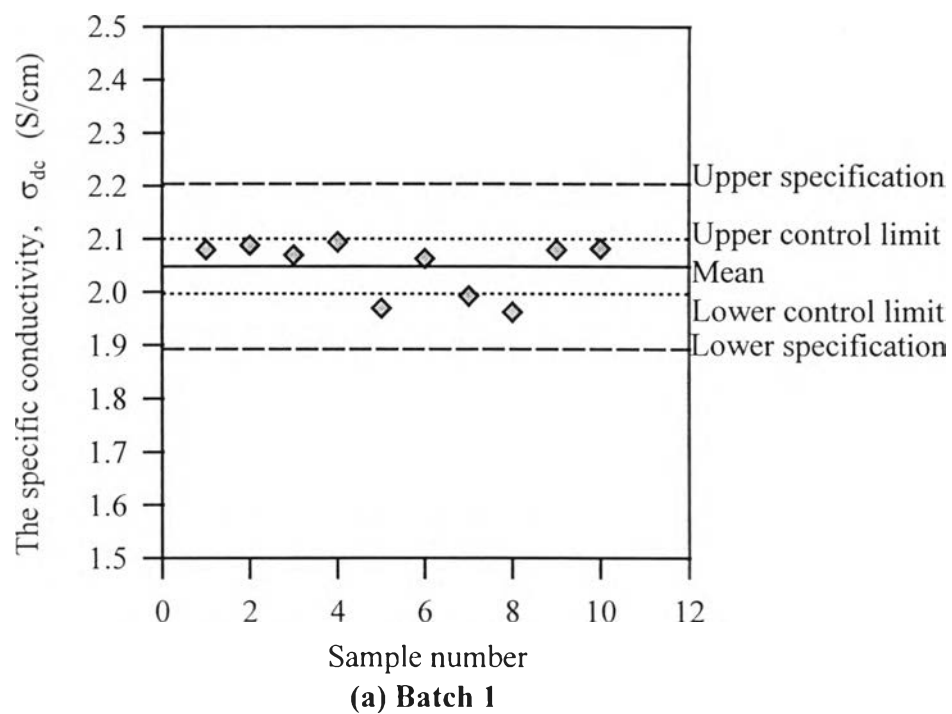


**Figure 3.9** X-bar charts of the specific conductivity for 0.30 M DBSA-doped polypyrrole films at 18 °C.

### 3.2.3 Effect of Applied Current on The Conductivity Response

In the constructed four-point probe detector, the applied current can be varied from 0 to 2.7  $\mu\text{A}$ . Therefore the effect of the applied current in this range on the conductivity response was studied. The conductivity of the DBSA polypyrrole films were observed in 1 atm of  $\text{N}_2$  atmosphere at 18  $^\circ\text{C}$ . Figure 3.10. shows the specific conductivity of DBSA polypyrrole films with various doping levels as a function of applied current. It is shown here that the applied current does not affect the specific conductivity at the applied currents ranging from 0.5 to 2.7  $\mu\text{A}$ . This is because the applied currents were very small and they cannot generate enough heat to influence the conductivity response. So, we decided to use the applied current of 2.7  $\mu\text{A}$  for studying the conductivity response in further work to minimize errors due to sensitivity of our voltmeter.

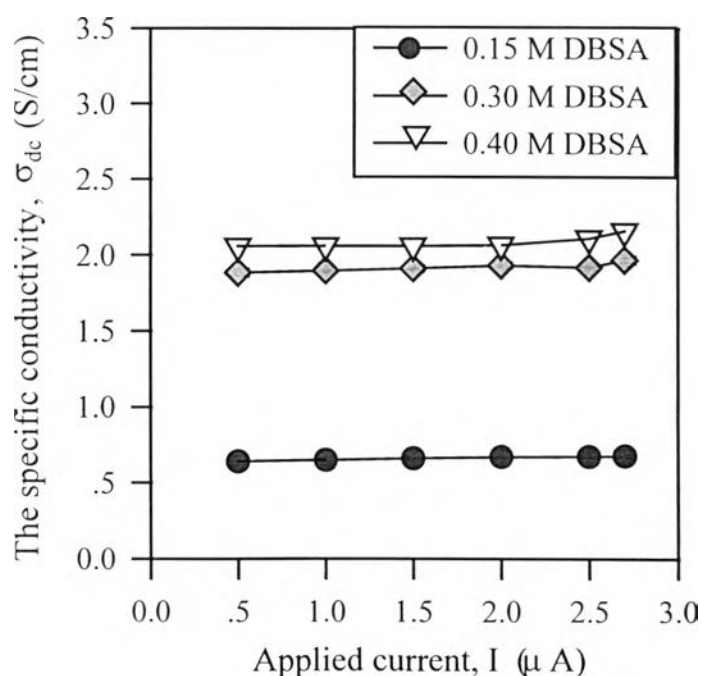


**Figure 3.10** Effect of the applied current on the specific conductivity of the DBSA-doped polypyrrole at 18  $^\circ\text{C}$ .

### 3.3 Electrical Conductivity

#### 3.3.1 Effect of Dopant Concentration

In this work, DBSA used as the dopant was varied from 0.15 M to 0.40 M. The conductivity of the DBSA polypyrrole films were observed by using the four-point probe detector with 2.7  $\mu\text{A}$  of applied current in 1 atm of  $\text{N}_2$  atmosphere at 18  $^\circ\text{C}$  as seen in Figure 3.11. The specific conductivity increases with the DBSA concentration. This result supports the FTIR and UV-VIS results which show the increase in the sulfate absorption and bipolaron absorption. We can argue that when we use a greater DBSA concentration, more DBSA particles can react with polypyrrole and then remove more electrons from polypyrrole chains. More positive charges occur in form of bipolaron state and then the higher conductivity follows. However, the specific conductivity seems to saturate at 0.35 M DBSA-doped polypyrrole.

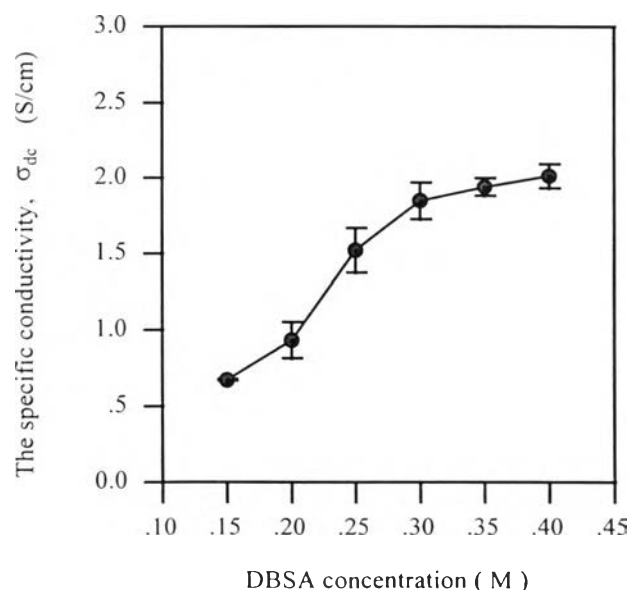


**Figure 3.11** Effect of DBSA concentration on the specific conductivity of the DBSA-doped polypyrrole films at 18  $^\circ\text{C}$  and 1 atm  $\text{N}_2$ .

### 3.3.2 Effect of Testing Temperature

The specific conductivity of the DBSA-doped polypyrrole films was studied as a function of testing temperature. The conductivity was observed by the four-point probe detector with 2.7  $\mu\text{A}$  of applied current in 1 atm of  $\text{N}_2$  atmosphere. Figure 3.12 represents the plot of the specific conductivity of polypyrrole films with various doping levels as a function of testing temperature ranging from 18  $^\circ\text{C}$  to 70  $^\circ\text{C}$ . The specific conductivity of 0.20 M - 0.40 M DBSA-doped polypyrrole films shows a general feature of a conductive polymer, the d.c. conductivity increases with temperature, whereas in the case of 0.14 M and 0.15 M DBSA-doped polypyrrole films, the opposite effect occurs at low temperatures in the range of 20  $^\circ\text{C}$  - 32  $^\circ\text{C}$ , followed by an increase in conductivity at higher temperature. The phenomena can be divided into two parts as follows :

a) For 0.20 M - 0.40 M DBSA-doped polypyrrole films, the d.c. conductivity increases with temperature. This can be described by the higher mobility of existing of charges carriers and creation of new charge carriers in polypyrrole chains, hence the increase in the d.c. conductivity based on the general relationship expressed in Equation 1.3, are a result of thermal excitation of charges carriers. *As Stuke et al. (1970)* emphasized, the plot of  $\ln \sigma_{\text{dc}}$  versus  $1/T$  gives a good straight line over a considerable range of temperature. The electrical conductivity is a negative exponential function of inverse temperature and can be written by the general equation :

$$\sigma_{\text{dc}}(T) = \sigma_0 \exp\left(\frac{-E_a}{k_B T}\right) \quad (3.2)$$

where  $\sigma_{\text{dc}}(T)$  is the specific conductivity,  $\sigma_0$  is a constant ,  $E_a$  is the activation energy for conduction,  $k_B$  is the Boltzmann constant and  $T$  is the absolute

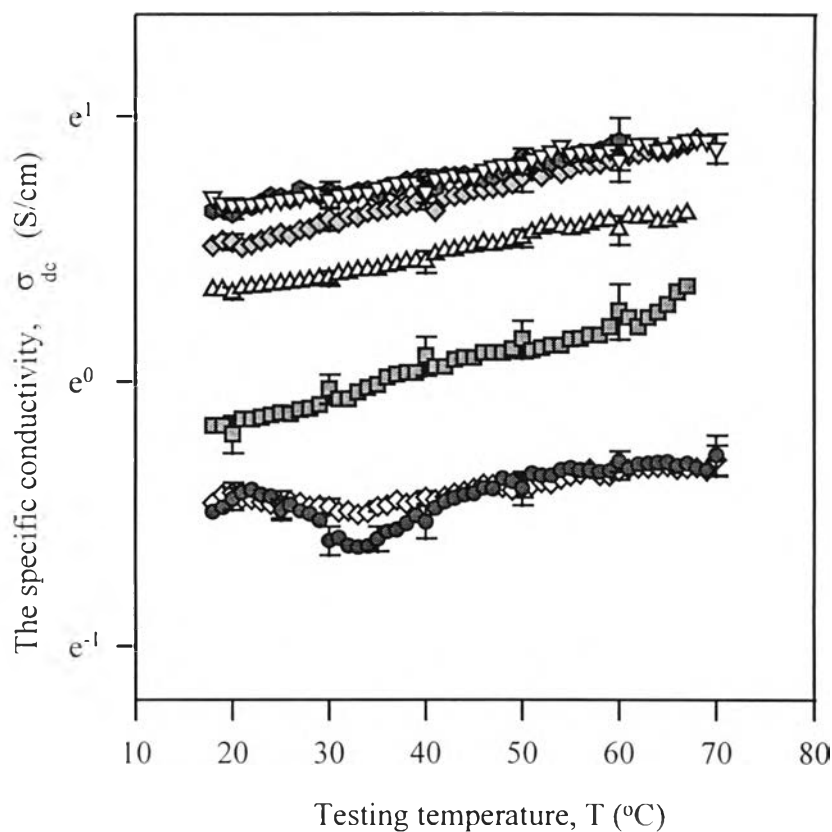


**Figure 3.12** Plot of  $\sigma_{dc}$  versus  $T$  for the DBSA-doped polypyrrole films with (a) 0.14 M DBSA,  $\diamond$ , (b) 0.15 M DBSA,  $\bullet$ , (c) 0.20 M DBSA,  $\blacksquare$ , (d) 0.25 M DBSA,  $\triangle$ , (e) 0.30 M DBSA,  $\diamond$ , (f) 0.35 M DBSA,  $\bullet$ , (g) 0.40 M DBSA,  $\nabla$ .

temperature. The activation energy of 0.20 M DBSA - 0.40 M DBSA-doped polypyrrole films can be calculated from the slope of  $\ln \sigma_{dc}$  against  $1/T$  as shown in Figure 3.13. and tabulated in Table 3.4. We can see that the activation energy decreases with the doping level. These results agree with those of *Berthet et al. (1987)* who reported that during doping reaction the incremental  $\text{NO}_2$  concentration, acted as dopant, not only increased the room temperature conductivity but also resulted in a general decrease of the slopes of the  $\ln \sigma_{dc}$  versus  $1/T$  plots.

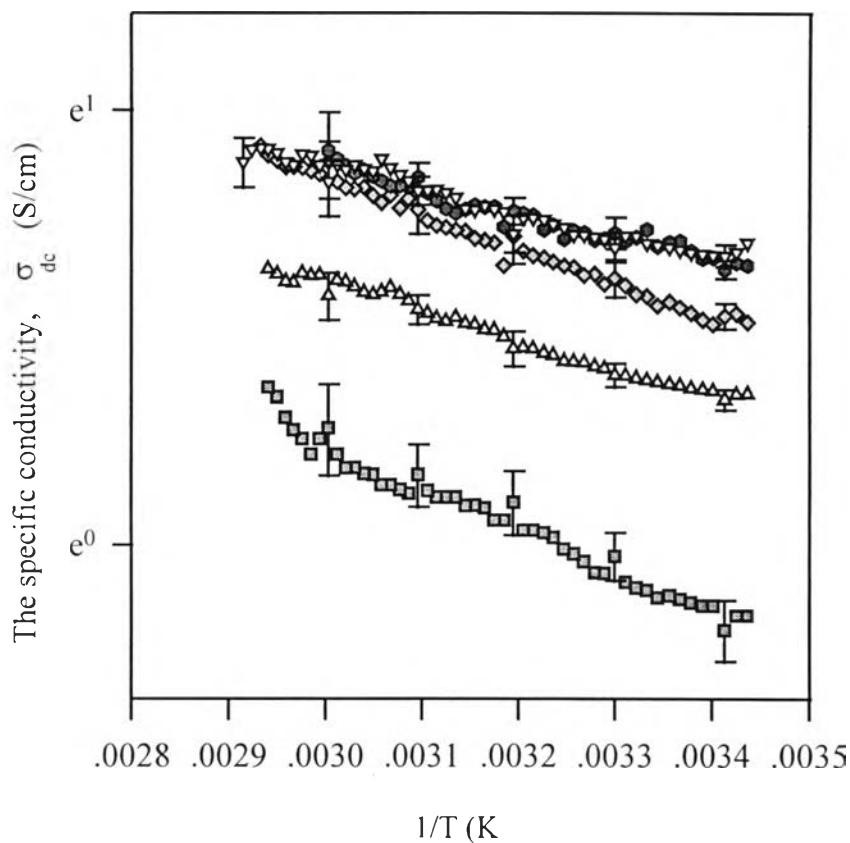


**Figure 3.13** Plot of  $\ln \sigma_{dc}$  versus  $1/T$  for the DBSA-doped polypyrrole films with (a) 0.20 M DBSA,  $\square$ , (b) 0.25 M DBSA,  $\Delta$ , (c) 0.30 M DBSA,  $\diamond$ , (d) 0.35 M DBSA,  $\bullet$ , (e) 0.40 M DBSA,  $\nabla$ .

**Table 3.4** The activation energy for various DBSA concentration in the temperature range : 18 °C to 70 °C

DBSA concentration (M)	The activation energy, $E_0$ ( eV )
0.20	0.0846
0.25	0.0660
0.30	0.0702
0.35	0.0476
0.40	0.0444

The Mott variable range hopping (VRH) model [Mott *et al.* (1979)] was proposed for describing the mechanism of charge carrier transport. It is a form of hopping transport which results when an electron may hop to a distant site instead of just a neighboring site if the energy difference between its current site and the distant site is smaller than the difference between its current site and the neighboring site. The specific conductivity was plotted following the general form of the temperature-dependent conductivity of Mott's model as described in Equation 3.3 :

$$\sigma = \sigma_0 \exp \left[ - \left( \frac{T_0}{T} \right)^{1/d+1} \right] \quad (3.3)$$

where  $\sigma_0$  is a constant,  $d$  is the dimensionality and, for three dimensional system,  $T_0 = c / k_B N(E_F) L^3$  ( $c$  is the proportionality constant,  $k_B$  the Boltzman constant,  $N(E_F)$  the density of states at Fermi level and  $L$  the localization length). For a one dimensional chain ( $d = 1$ ) the localization of charge carriers arises for even weak disorder because of quantum interference of static back-scattering. In contrast, strong disorder (the mean free path is comparable with the Fermi wavelength) is required for localization in three-dimensional system ( $d = 3$ ). However both 1-D and 3-D VRH model provide a good fit to our data through the entire temperature range as shown in Figure 3.15. This is because there may be no effect of the dimensionality on the conductivity or the temperature range used was too small.

b) In the case of 0.14 M and 0.15 M DBSA-doped polypyrrole films, the conductivity response can be divided into two regimes (Figure 3.12a and Figure 3.12b). First, the conductivity response in the temperature range of 33 °C - 70 °C represents the same trend as higher doping level mentioned above. Second, at the low temperature range (18 °C - 32 °C), it is very interesting to find that the conductivity response shows metal-like

behavior where the specific conductivity decreases with temperature. We are not sure about the actual reasons. However we can propose some idea and models for this situation by considering some previous works and the results of the morphology study because the conducting polymers generally display a rich variety in their morphology. From the morphology, results the low-doped polypyrrole contains 3D random coil-like structures whereas the higher-doped polypyrrole shows fibril structures. In the low temperature range, when the temperature increases the 3D random coil structure of the low doped polypyrrole will expand and increase the free volume as can be seen in Figure 3.14. The increase in free volume causes difficulty for interchain transport to occur, so the conductivity goes down. In the case of highly-doped polypyrrole, chain expansion can hardly affect the interchain transport, since they have already been expanded by the repulsing electrostatic effect. However as seen in Figure 3.12, the increase in conductivity response still appears. *Bredas et al. (1984)* indicated that polypyrrole, poly(p-phenylene) and polythiophene possess a nondegenerate ground state since their ground states correspond to a single geometric structure which is aromatic-like. A quinoid-like resonance structure can be envisioned but has higher total energy (Figure 3.16). They showed that

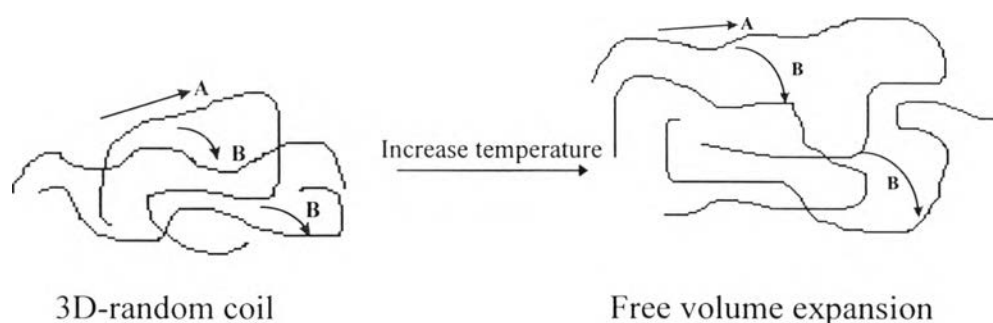


**Figure 3.14** A possible model for low-doped polypyrrole chains when temperature increases.



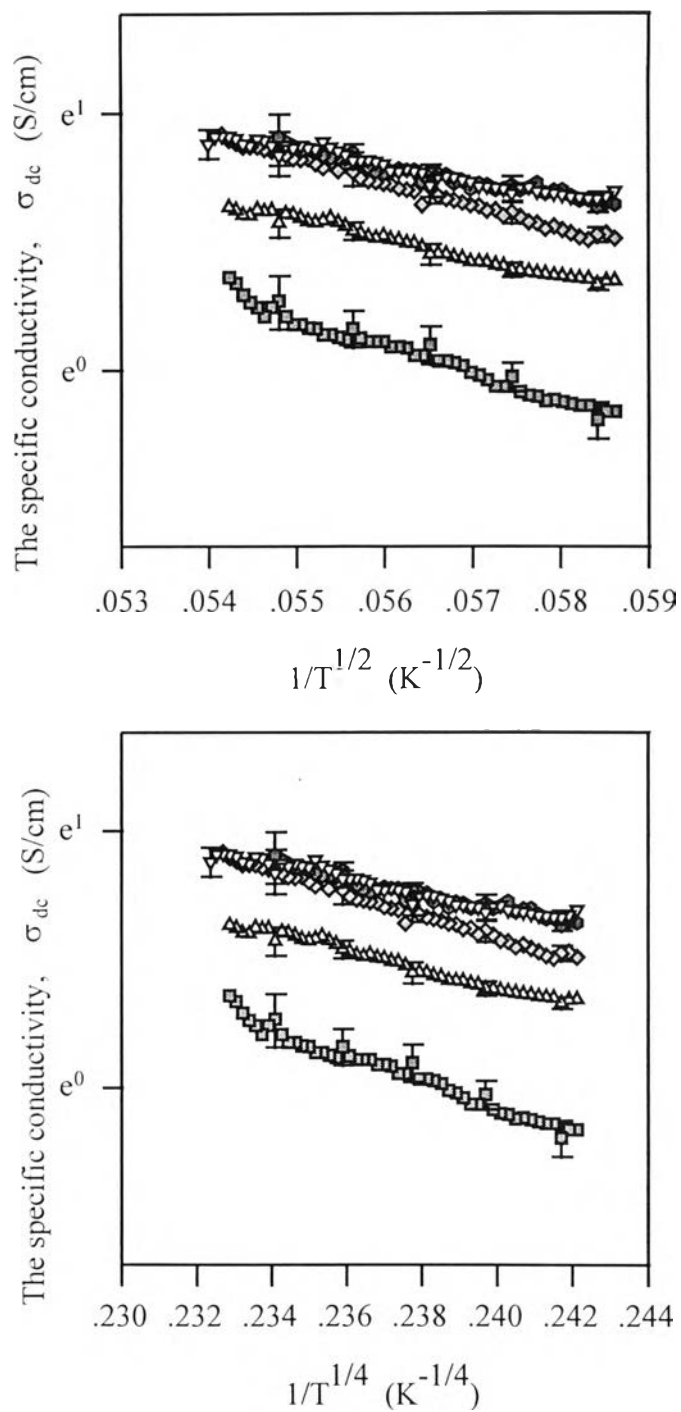


**Figure 3.15** Plot of  $\ln \sigma_{dc}$  versus (A)  $1/T^{1/2}$  and (B)  $1/T^{1/4}$  for the DBSA-doped polypyrrole films with (a) 0.20 M DBSA,  $\blacksquare$ , (b) 0.25 M DBSA,  $\blacktriangle$ , (c) 0.30 M DBSA,  $\blacklozenge$ , (d) 0.35 M DBSA,  $\blacklozenge$ , (e) 0.40 M DBSA,  $\blacktriangledown$ .

the quinoid structure has a lower ionization potential and a larger electron affinity than the aromatic structure. From this reason, we can suggest that the higher-doped polypyrroles exhibit more quinoid structure and the larger electron affinity, meaning that electrons can be easier removed from higher doped polypyrrole chains in comparison with the lower-doped polypyrrole chains and then more new charge carriers can be created. These new charge carriers cause the increase in the conductivity. This is the possible reason why in the low temperature range, the specific conductivity increases with temperature for the highly-doped polypyrroles whereas the specific conductivity decreases with temperature for the lower-doped polypyrroles.

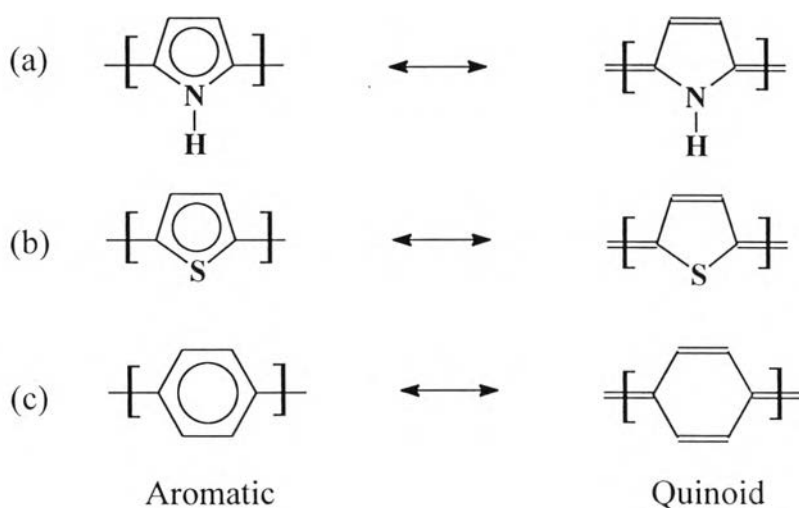


**Figure 3.16** Aromatic (ground state) and quinoid-like geometric structures for (a) polypyrrole, (b) polythiophene, (c) poly(p-phenylene).

### 3.3.3 Effect of Exposure Time to SO<sub>2</sub>

The specific conductivity of the DBSA-doped polypyrrole films was studied as a function of exposure time to SO<sub>2</sub>. The conductivity was observed by the four-point probe detector with 2.7  $\mu$ A of applied current at 18 °C in 1 atm of 2500 ppm SO<sub>2</sub> atmosphere. Figure 3.17 illustrates the plot of the specific conductivity of polypyrrole films with various doping levels versus exposure time to SO<sub>2</sub>. It can be seen that the specific conductivity increases with exposure time. The reason is SO<sub>2</sub>, an electron acceptor gas, can remove some electrons from polypyrrole chains, so the holes or positive charges are created. The positive charges along the polypyrrole chains act as charge carriers for conduction therefore the conductivity increases. From Figure 3.17 we also observe that the rate of conductivity changes for various doping levels, observed from the slope in an initial stage of the gas exposure, are different. The higher doping level show a higher rate of conductivity change and become saturated in a lesser amount of time. For the polypyrrole with has higher electron affinity because of more quinoid-like structure, SO<sub>2</sub> can easily remove electrons from polypyrrole chains in an initial stage. The adsorption sites along polypyrrole chains are compensated by sulfate anions and become saturated faster than the lower-doped polypyrroles.

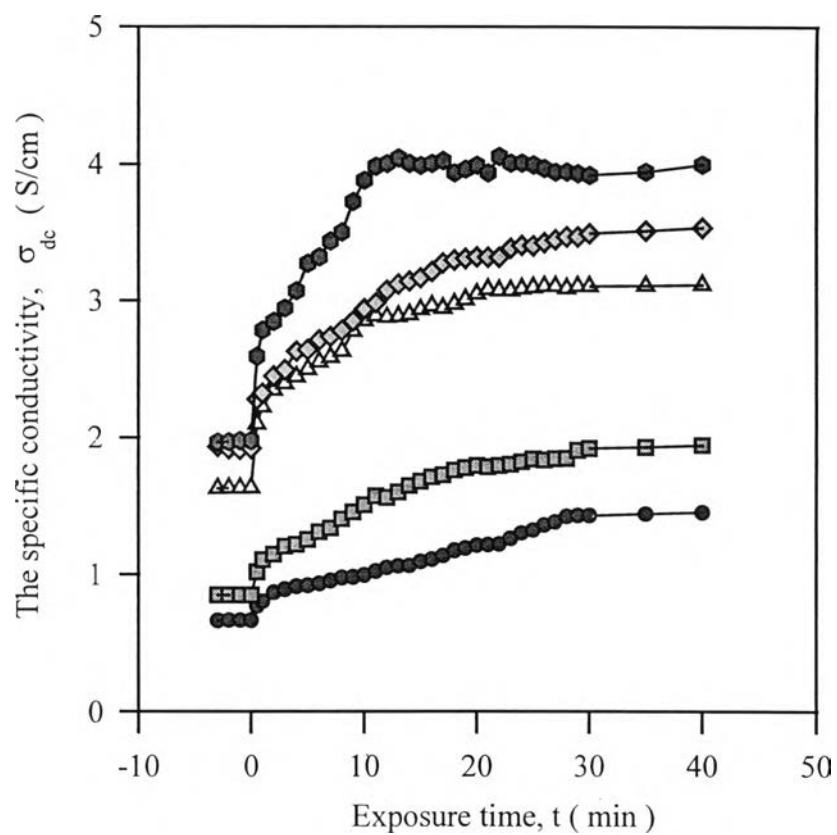


**Figure 3.17** Effect of exposure time to 2500 ppm  $\text{SO}_2$  at 18 °C for DBSA doped polypyrrole films with (a) 0.15 M DBSA, ●, (b) 0.20 M DBSA, ■, (c) 0.25 M DBSA, △, (d) 0.30 M DBSA, ◇, (e) 0.35 M DBSA, ◈.

### 3.3.4 Effect of SO<sub>2</sub> concentration

The dependence of the DBSA-doped polypyrrole films conductivity on SO<sub>2</sub> concentration was investigated for gas sensor application. The conductivity was observed by the four-point probe detector with 2.7 μA of applied current at 18 °C in 1 atm of various SO<sub>2</sub> concentration. Figure 3.18 displays the plots of the specific conductivity of the DBSA-doped polypyrrole films at various doping levels against log SO<sub>2</sub> concentration based on the general log's law as expressed in Equation 3.4

$$\sigma_{dc} = a \log c_{SO_2} \quad (3.4)$$

where  $\sigma_{dc}$  is the specific conductivity,  $c_{SO_2}$  is SO<sub>2</sub> concentration and  $a$  is constant. The relation is linear within the SO<sub>2</sub> concentration range of 500 - 2500 ppm. We thus demonstrate that the DBSA-doped polypyrrole films can be used as SO<sub>2</sub> sensor within this concentration range. Considering that the slopes of the various doping levels are different, the doping level seems to play an important role in determining the gas sensitivity of DBSA-doped polypyrrole films. In order to consider the sensitivity of the sensor, the data from Figure 3.18 are replotted as conductivity change, calculated by Equation 3.1, versus SO<sub>2</sub> concentration and then shown in Figure 3.19. It seems to illustrate that the highest sensitivity of the sensor is at 0.15 M DBSA-doped polypyrrole because it shows the largest conductivity change when compared with the higher-doped polypyrrole.

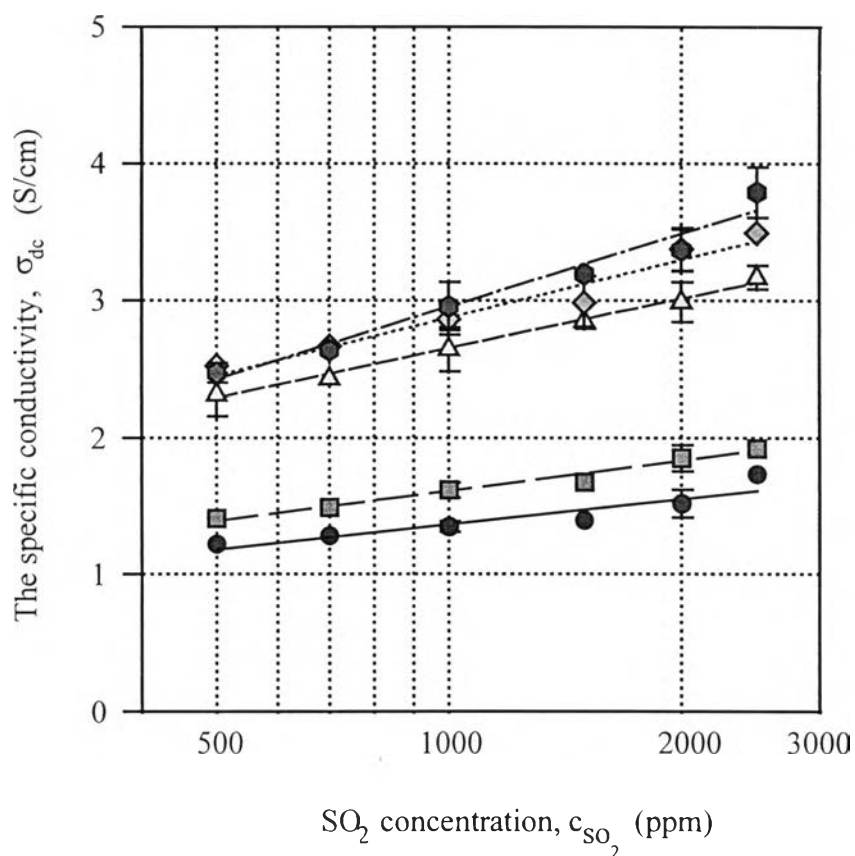


**Figure 3.18** Effect of  $\text{SO}_2$  concentration at 18 °C for DBSA-doped polypyrrole with (a) 0.15 M DBSA, ●, (b) 0.20 M DBSA, ■, (c) 0.25 M DBSA, △, (d) 0.30 M DBSA, ◇, (e) 0.35 M DBSA, ⬠.

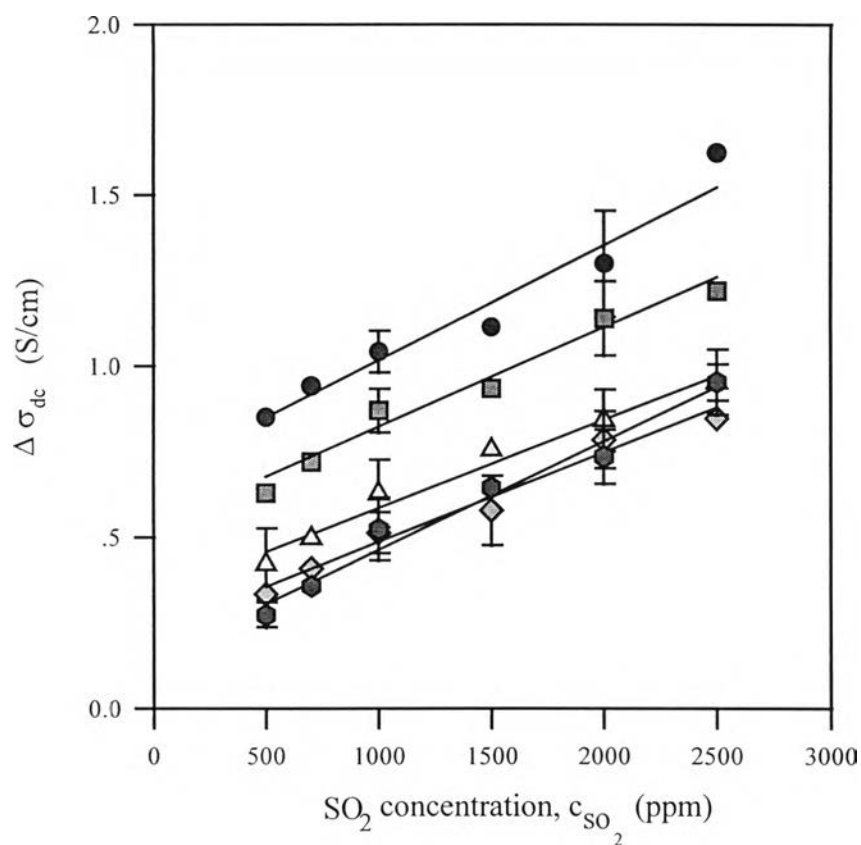


**Figure 3.19** Plot of the specific conductivity change *versus* SO<sub>2</sub> concentration at 18 °C for DRSA-doped polypyrrole with (a) 0.15 M DBSA, ●, (b) 0.20 M DBSA, ■, (c) 0.25 M DBSA, △, (d) 0.30 M DBSA, ◇, (e) 0.35 M DBSA, ⬡.

### 3.3.5 Effect of Testing Temperature in SO<sub>2</sub> Atmosphere

The effect of testing temperature on the specific conductivity of DBSA-doped polypyrrole when exposed to SO<sub>2</sub> atmosphere is an important point for portable gas sensor investigation, therefore the specific conductivity of DBSA-doped polypyrrole films was detected at various temperatures by the four-point probe detector with 2.7  $\mu\text{A}$  of applied current in 1 atm of 1000 ppm SO<sub>2</sub>. Figure 3.20 shows the plots of the specific conductivity of the 0.15 M, 0.25 M, and 0.35 M DBSA-doped polypyrrole films at various temperatures. They seem to display the same trend; their specific conductivities increase with temperature in the range of about 18 °C to 50 °C and decrease at the higher temperature. The increasing conductivity in the first range is a result from the creation of new charge carriers in the polypyrrole chains because of the electron attraction of SO<sub>2</sub> and the increment in charge carrier mobility because of increasing temperature. However, higher temperature (50 °C to 70 °C), the specific conductivities decrease with increasing temperature; this may be caused by the desorption of SO<sub>2</sub> molecules from polypyrrole chains. When temperature increases, the expansion of polypyrrole film occurs, resulting in larger free volume, and greater SO<sub>2</sub> mobility, so they can desorb from polypyrrole chains more easily.



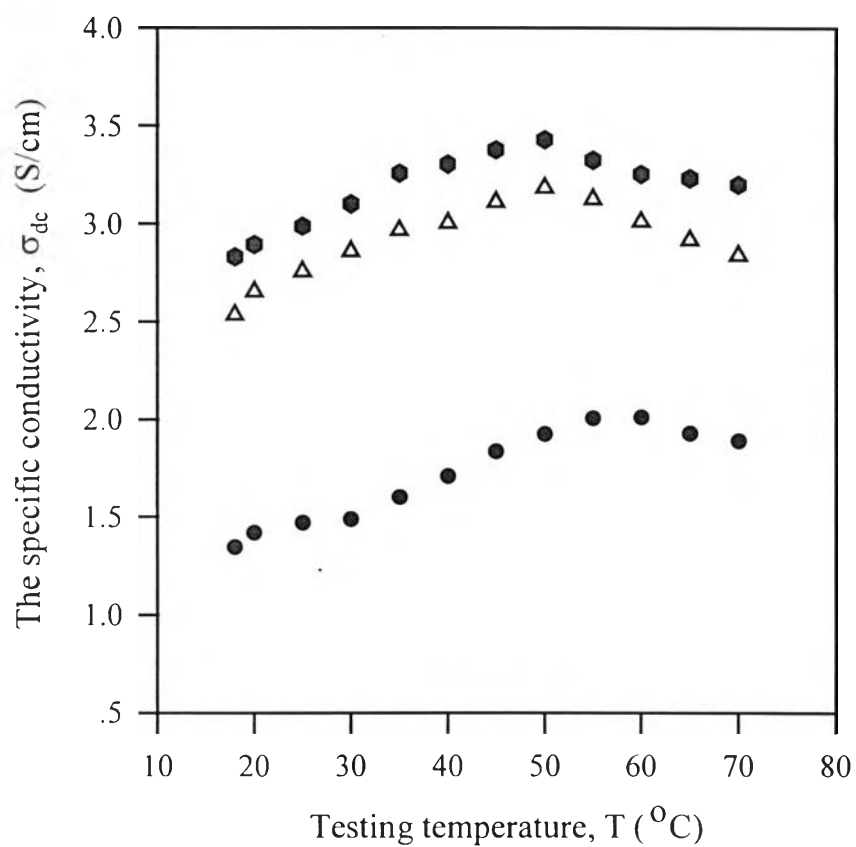


**Figure 3.20** Plot of the specific conductivity *versus* temperatures in 1000 ppm SO<sub>2</sub> atmosphere of the DBSA-doped polypyrrole films with (a) 0.15 M DBSA, ●, (b) 0.25 M DBSA,  $\Delta$ , (c) 0.35 M DBSA,  $\hexagon$ .